



## COPPER PLATING CORROSION STUDY IN CERTAIN ENVIRONMENTS

A.M. CANTARAGIU<sup>1</sup>, M.D. GAVRIL (DONOSE)<sup>1</sup>, D.C. VLADU (RADU)<sup>1</sup>,  
C. GHEORGHIES<sup>2</sup>, N. TIGAU<sup>2</sup>, C.M. CANTARAGIU<sup>3</sup>

<sup>1</sup>PhD students, <sup>2</sup>Faculty of Sciences and Environment, Chemistry, Physics and Environment Department

<sup>3</sup>Student, Faculty of Metallurgy, Materials Science and Environment

„Dunarea de Jos” University of Galati

email: [cantaragiu\\_alina@yahoo.com](mailto:cantaragiu_alina@yahoo.com)

### ABSTRACT

*Copper plating was performed on nickel substrate by means of the potentiostatic electrodeposition method from a sulphate electrolyte solution. The copper coatings morphology was studied by means of the optical and electronic scanning microscopy techniques. The uniform electrodeposited films have a thickness of about 15 μm measured in cross-section. The corrosion behaviours of nickel substrate and copper films in different corrosive environments were studied. The corrosion study was performed by means of the linear polarisation method in four acid environments: 0.5 M H<sub>2</sub>SO<sub>4</sub>, HCl, HNO<sub>3</sub> and glacial CH<sub>3</sub>COOH. From the recorded Tafel curves it was possible to obtain some information about the corrosion rate and the polarization resistance. In order to confirm these results, the gravimetric parameter was calculated by means of the “mass loss” method. By means of the X-ray diffraction analysis, the crystallographic structure of the specimens before and after corrosion was revealed. By means of the spectrophotometer device, the optical properties of the specimens were analysed.*

KEYWORDS: electrodeposition, copper plating, corrosion, nickel substrate

### 1. Introduction

In recent years, copper has replaced aluminum as a metal for interconnects in electronic industry. Copper thin films are also used in the multilayer sandwiches of GMR hard disk read heads.

Among various methods of copper thin film deposition onto substrates, such as PVD, CVD, and sputtering, the electrochemical methods (electrolytic) have proven to be the least expensive, highly productive and readily adoptable [1].

Copper electrodeposition mechanisms have been studied in two chemical systems: the acidic without complexation [1] and the basic one, requiring the presence of buffering [2-4] and complexing reagents.

For obtaining the copper from the negative electrode some processes can be related, such as precipitation, extraction, or electrodeposition [5,6]. One of these is the electrochemical process where electrodeposition baths are made, with or without the addition of complexing additives to increase efficiency.

An important characteristic of these electrodeposits is the morphology, where the

electrodeposit growth can be related to the nucleation process (in two or three dimensions).

*Searson et al.* [7] studied the morphology and kinetics for copper nucleation during the electrodeposition in strongly acid media (pH~1.0) without additives. They observed that copper electrodeposition occurs at potentials over -0.04V and consists of the direct reduction of Cu<sup>2+</sup> ions to metallic copper. They also observed that the current increases at slower rates related to the decrease in the quantity of ions from the bulk to the interface, showing a diffusion reaction-controlled process. For more negative potentials, the growth of nuclei was controlled by diffusion.

*Zangari et al.* [8] observed that, at pH of 2.5, the copper morphology shows a dendritic form and then forms clusters in the electrodeposit.

*Pesic and Grujicic* [4] correlated the nucleation process of copper electrodeposition and morphology and observed that at pH values over 3 the nucleation process was progressive (threedimensional growth) and, below this value, the model tended to an instantaneous nucleation, related to a bi-dimensional growth.

*Pasquale et al.* [9] studied the morphology of copper electrodeposits. They observed that the bath composition (preferably pH values) has a significant influence on the copper morphology, with well-formed grains and nuclei being formed in acid media.

Otherwise, at higher pH values, *Gabrielli et al.* [10] observed that copper electrodeposition formed small dendrites related to a copper metallic layer and another oxide layer, normally Cu<sub>2</sub>O.

*Nikolitic et al.* [11] observed that the hydrogen co-deposition with metallic copper was related to a three-dimensional growth due to the porous morphology [12].

The aim of this investigation was to obtain copper films onto nickel substrate by means of the potentiostatic electrochemical deposition method. Also, the corrosion behaviour of these deposits in acid environments (0.5M H<sub>2</sub>SO<sub>4</sub>, HCl, HNO<sub>3</sub> and glacial CH<sub>3</sub>COOH) was studied. Nickel surface was copper coated to evaluate the properties of the un-coated and coated surface during the corrosion process. These properties refer to the microstructural feature analysed by the optical and scanning electron microscopy (SEM), energy dispersive X-ray (EDX), as well as by X-ray diffraction (XRD) techniques where the corrosion resistance enhanced. The increased corrosion resistance results in improved protective coating performance that can be used as a hard surface on softer substrates.

## 2. Materials and methods

### 2.1. Materials

The copper chemical powder was purchased from commercial sources and has the highest purity available. The copper films have been electrodeposited onto nickel substrate from sulphate electrolyte solution having the composition presented in Table 1 [4,14].

**Table 1.** Copper plating bath composition and working conditions (no magnetic stirring)

CuSO <sub>4</sub> ×5H <sub>2</sub> O	0.8 M
H <sub>2</sub> SO <sub>4</sub>	0.55 M
HCl	3.26×10 <sup>-3</sup> M
pH	1.7
T	50°C
Acid environments	0.5 M H <sub>2</sub> SO <sub>4</sub> , HCl, HNO <sub>3</sub> , CH <sub>3</sub> COOH

Before the electrochemical study, the samples were mechanically polished with fine grit SiC paper. Afterwards, the polished substrates were carefully chemically degreased with acetone and alcohol, etched with 1:10 HNO<sub>3</sub>:H<sub>2</sub>O, rinsed with distilled water and then, dried in air before their immersion in the electrolyte.

### 2.2. Methods and instruments

A standard three electrode system (electrochemical cell from Pyrex glass) with a cell (Fig. 1) volume of 100 mL was used to perform the electrochemical investigations at 50°C temperature. Temperature was controlled with a thermostat (model VEB MLW Prufgerate-Werk Medingen/Sitz Freital). An Ag/AgCl saturated electrode (SCE) served as the reference electrode (RE), and the counter electrode (CE) was a platinum sheet. A plate-shaped working electrode, WE, was made of nickel. The WE electroactive area was 2.5 cm<sup>2</sup>. The electrolyte pH was recorded by means of Consort C931 equipment. Also, before and after deposition, the samples weight was measured using an electronic balance (model ESJ200-4).

The coatings preparation and corrosion behaviour were carried out potentiostatically with a potentiostat/galvanostat VoltaLab10 interfaced with VoltMaster4 software for data acquisition and analysis [15].



**Fig. 1.** The experimental setup

Potentiodynamic polarisation curves of the deposited films were measured from - 500mV toward the anodic direction of 500mV, with a scan rate of 50mV/s. The corrosion behaviour of deposited films

has been observed by introducing them in different corrosive environments: 0.5M H<sub>2</sub>SO<sub>4</sub>, HCl, HNO<sub>3</sub> and glacial CH<sub>3</sub>COOH. The same electrodes presented above were used in this case. The exposure corrosion

time was one hour. The linear polarisation (Tafel curves) was used as method to study the corrosion behaviour. The corrosion rate is automatically calculated by specialized computer software using the Randles-Sevcik equation (1). Before and after each experiment the samples weight was measured by means of analytical balance. The mass losses ( $\Delta m_{corr}$ ) and penetration index ( $p$ ) values are shown in Table 2.

### 2.3. Morphology and structural characterization of metallic samples

The surface morphological features of the metallic specimens were examined by means of SEM measurements. Also, the chemical composition was achieved by means of EDX measurements. The micrographs and chemical compositions were registered using Quanta 200 Philips FEI Company device.

The crystallographic characteristics of the samples were analysed through the XRD using DRON-3M diffractometer. The XRD spectra were recorded at room temperature, X-ray diffractometer

using the  $\text{CoK}_\alpha$  radiation ( $\lambda = 1.79\text{\AA}$ ) in 2 $\theta$  configuration ranged between 30 and 70°, at 40 kV tension and 30 mA current intensity with a scanning speed of  $0.02^\circ \text{ min}^{-1}$  and acquisition time of 1 s/step.

By means of the interaction between a polychromatic beam and a copper film coated its behaviour was examined by reflectance measurements recorded by means of Perkin Elmer (type Lambda) 35 UV-VIS Spectrophotometer with double beam in the spectral range of 190÷1100nm.

### 3. Results and discussion

The appearance of nickel and copper coatings is analysed by means of the optical microscope at 500× magnification (Fig. 2). Obviously, a colour difference between two optical images of nickel substrate and copper coating can be seen. The polishing traces from nickel substrate with a grey colour (Fig. 2a) are compared to the reddish colour and spots from copper the deposit (Fig. 2b).

The copper crystalline grains can be observed.

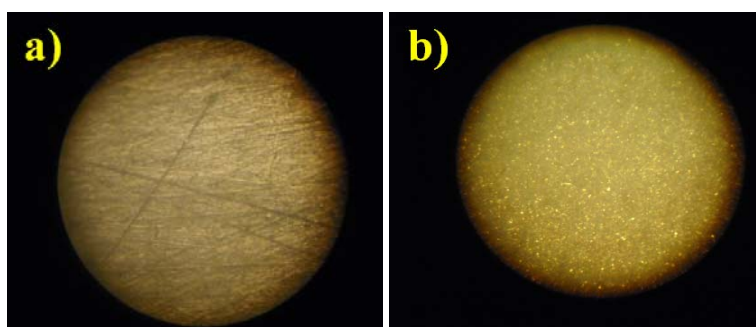
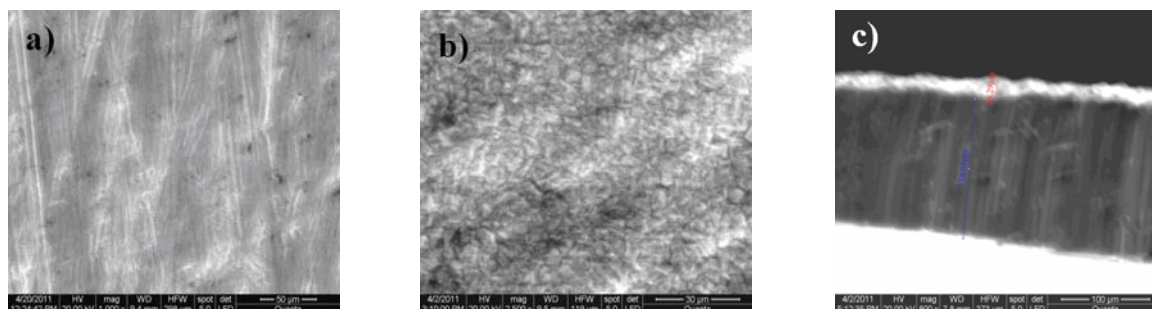
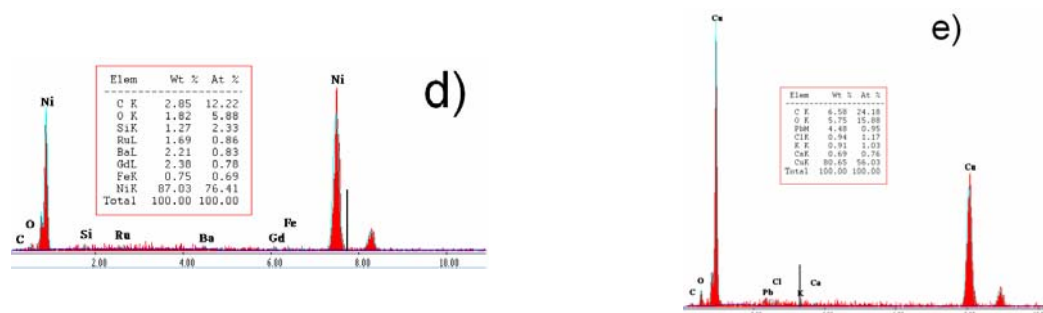


Fig. 2. The optical microstructure of a) nickel substrate and b) copper film before the corrosion test (500×)

The above images are confirmed by the SEM micrographs (Fig. 3). Fig. 3a corresponds to the nickel substrate with the polishing direction traces, after the pre-treatment procedure. The chemical composition (Ni – 87wt %) of the substrate is confirmed by EDX analysis (Fig. 3d). The copper film shows the

tetrahedral crystalline grains (Fig. 3b). The grain size is relatively faint and shows an excellent uniformity<sup>16</sup>. The EDX spectrum (Fig. 3e) shows the chemical composition of copper film deposited (Cu – 80wt %). Also, the thickness film was measured in cross section and it is around 25µm (Fig. 3c).





**Fig. 3.** Surface morphology of: a) nickel substrate; b) copper film; c) cross-sectioned copper coating obtained from a sulphate electrolyte (from top-down) at 50°C; d) EDX spectrum of nickel substrate and e) copper film

The corrosion rates (Table 2) were achieved by means of the “mass loss method” [17,18], in static regime at room temperature and calculated based on equation (1):

$$V_{corr} = \frac{\Delta m}{S \cdot t} \quad (1)$$

where:  $V_{corr}$  = gravimetric index [ $\text{g}/\text{m}^2\text{s}$ ];  $\Delta m$  = weight loss (before and after the corrosion test) by corrosion [g];  $S$  = corroded surface area [ $\text{m}^2$ ];  $t$  = corrosion time [s].

The average depth of the composite corrosive destruction is calculated using the formula (2):

$$p = \frac{V_{corr}}{\rho} \cdot 8.76 \quad (2)$$

where:  $p$  = penetration index [ $\text{mm}/\text{y}$ ];  $V_{corr}$  = gravimetric index [ $\text{g}/\text{m}^2\text{s}$ ];  $\rho$  = composite film density [ $\text{g}/\text{cm}^3$ ].

The results are presented in Table 2.

**Table 2.** Corrosion behaviour of copper coatings onto nickel substrates immersed in acid solutions

Sample	$\bar{d}$	$\Delta m_{corr}$	$V_{corr}$	$p$	Resistance group	Estimate note
	[ $\mu\text{m}$ ]	[g]	[ $\text{g}/\text{cm}^2\text{h}$ ]	[ $\text{mm}/\text{y}$ ]		
1. with film	25	0.0516	-	-	-	-
2. with film in $\text{H}_2\text{SO}_4$		-0.0024	<b>0.096</b>	0.094	Very stable	2-3
3. with film in HCl		-0.0007	0.016	0.016	Very stable	2
4. with film in $\text{HNO}_3$		-0.002	0.047	0.046	Very stable	2
5. with film in $\text{CH}_3\text{COOH}$		0	0	0	Perfect stable	1

The copper growth is also affected by immersion in 0.5 M  $\text{H}_2\text{SO}_4$  environment (Fig. 4a) which change the surface morphology and texture. Regarding the values in Table 2, this environment is the most aggressive environment having the highest corrosion rate. Also, the higher weight difference shows that a great number of copper ions were reduced from the surface during the electrochemical corrosion. The surface is coated with a uniform oxide layer on the copper film. The copper surface has a lower instability in contact with  $\text{H}_2\text{SO}_4$  environment and the corrosion process is continuous. Also, this fact is confirmed by the EDX analysis (Fig. 4b). The sample insertion into a chloride solution (Fig. 4c) affects both the structure and morphology: the epitaxial growth on the nickel seed is favoured giving [111] and [200] textured layers; the grain size is slightly reduced and more uniform, with increased tendency to faceting and

formation of triangular based pyramids, related to [111] texture, also with truncated apex, indicative of weak interfacial inhibition. The chloride oxide compounds on the surface were observed (Fig. 4d).

A few corrosion microelements on the copper film were observed when the sample was electrochemical by tested into the  $\text{HNO}_3$  environment (Fig. 4e) [19]. The surface is instable inside the  $\text{HNO}_3$  atmosphere. Due to the iron ions (Fig. 4f) content from the substrate, the aggressive action of this environment could be explained.

The copper deposition immersed into the glacial  $\text{CH}_3\text{COOH}$  environment presented a high surface stability having zero value for  $\Delta m$ ,  $V_{corr}$  and  $p$  parameters (Table 2) and being perfectly stable as a resistance group.

The XRD technique has been used to identify the structure of copper thin films onto nickel

substrates in two corrosion environments (0.5M H<sub>2</sub>SO<sub>4</sub> and CH<sub>3</sub>COOH) (Fig. 5).

The electrodeposition from sulphate bath on nickel substrate (with (111) and (200) specific crystallographic planes) gives copper layers two crystallographic orientations. The copper thin films are crystalline. The growth features are not well

defined, apart from scattered square base pyramidal grains (Fig. 4c).

Compared to the database from the Reference Pattern the free energy of the surface-support-solution system allows the preferential growth of copper crystallites after the [111] and [200] crystallographic direction was observed.

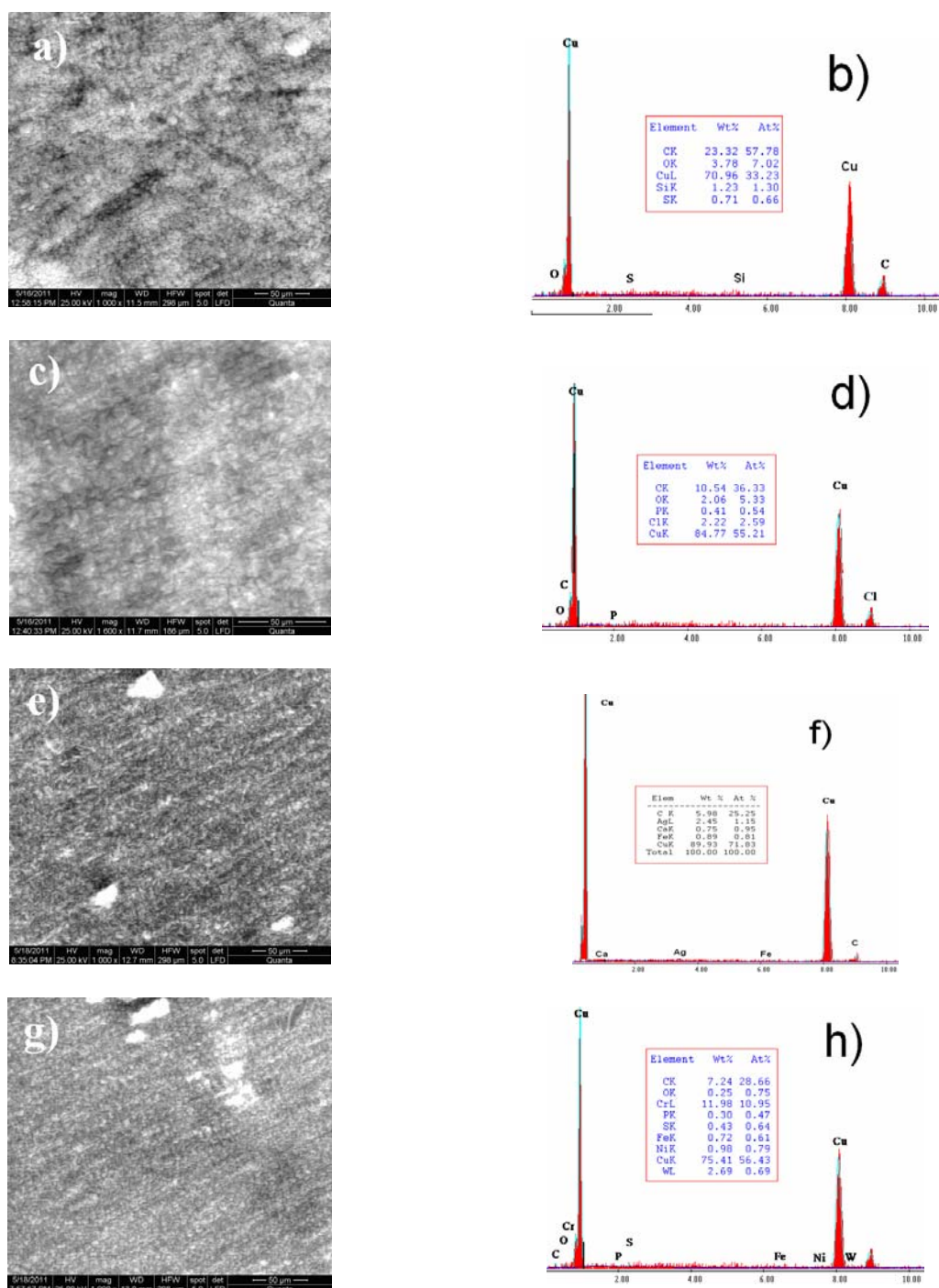
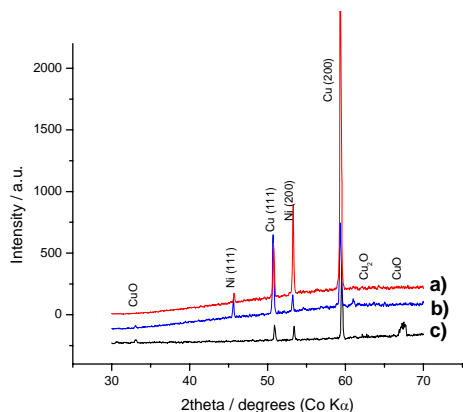


Fig. 4. SEM images and EDX spectra of copper coating corroded surfaces in: a-b) H<sub>2</sub>SO<sub>4</sub>; c-d) HCl; e-f) HNO<sub>3</sub> and g-h) CH<sub>3</sub>COOH

The XRD analysis shows the peaks corresponding to [111] and [200] characteristic directions of an *fcc* structure for electrodeposited copper, according to the Joint Committee on Powder Diffraction Standards (JCPDS) [18]. Direction [002] is related to the Cu<sub>2</sub>O structure [19].

The corrosion exposure to acid environment highlights the diffraction lines of oxide compounds (CuO, Cu<sub>2</sub>O) formed during the experiment (Fig. 5). Therefore, the crystalline network is rearranged; the internal stresses are reduced by testing the sample in acid conditions [17]. Also, the intensity peaks of copper decrease during the testing. The oxides operated like a protective layer against the aggressive environmental factor. This fact is confirmed by microscopical analyses.



**Fig. 5.** XRD patterns of a) copper coating and copper coating subjected to b) H<sub>2</sub>SO<sub>4</sub> and c) CH<sub>3</sub>COOH environments

Fig. 5 shows a higher background radiation for the corroded copper versus the copper. A presence of numerous point defects can be seen onto the corroded surfaces in comparison with the copper sample. The crystallographic defects can be the vacancies, interstitials or replaced atoms of the crystal lattice. In other words, the copper samples are crystalline materials but they are not perfect, the regular pattern of atomic arrangement is interrupted by crystallographic defects [18].

Fig. 6 is shown the polarization curves in the case of copper films immersed in all acid solution studied in this paper.

For CH<sub>3</sub>COOH environment the  $i_{corr}$  has the lower value while the  $R_p$  is high and the solution seems to have an inert activity. More corrosion resistance could be the CH<sub>3</sub>COOH solution. Then, increasing the corrosive activity of acid environment (H<sub>2</sub>SO<sub>4</sub>),  $i_{corr}$  and  $V_{corr}$  increase and the  $R_p$  is drastically decreased. This fact can be due to the impurities inclusion which exists into a metallic matrix.

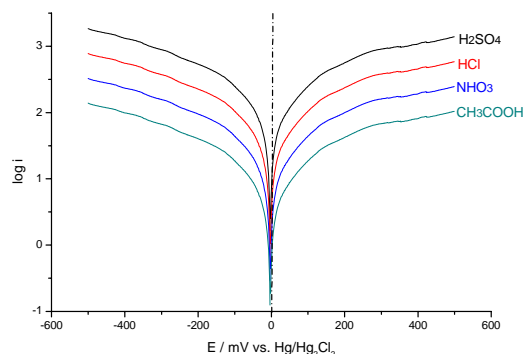


**Fig. 6.** Polarisation curves (50 mV/s) of copper deposition at 25°C in various acid environments

The HCl environment less corroded the surface and this fact means that the copper surface is quickly passivated. Thereby, these material surfaces could be classified in a very and perfectly stable resistance group due to the linear shape of the cathodic and anodic branches.

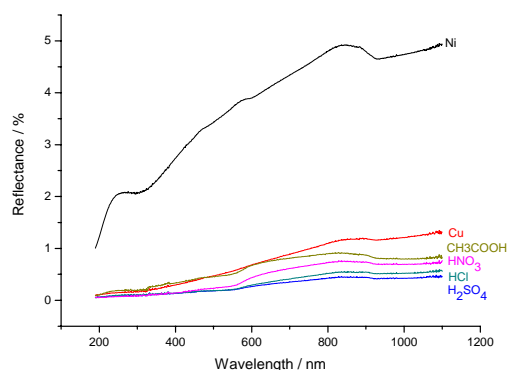


**Fig. 7.** UV-VIS-IR spectra of nickel substrate, copper film and copper subjected to acid environments

The curve in Fig. 7 corresponding to nickel indicates the formation of an inverse peak more evidently than those in the case of copper. This fact means that a minimum value of reflectance ( $R \approx 2$ ; 4.5%) appears at a maximum value of absorbance [20].

Increasing the wavelength increases the nickel surface capacity to reflect the light. The energy which is not adsorbed is reflected, being measured by means of the spectrometer. The amount of energy adsorbed can be easily determined by inspecting dips in the reflectance spectrum. Thereby, the nickel surface (linear shape of spectrum) is highly reflective in VIS region. For a thin and uniform copper layer appearance a linear shape curve was achieved having a good capacity to reflect the light. All copper deposition tested in the acid solution are good adsorber materials in VIS region due to the microelements presence on the surface.



#### 4. Conclusions

- ✓ The corrosion behaviour of copper deposits immersed in acid environments was investigated using the linear polarization method.
- ✓ The electrochemical parameters were calculated by means of the gravimetric method and linear polarisation method.
- ✓ The free energy of the surface-support-solution system allows the preferential growth of copper crystallites after the [111] and [200] crystallographic direction was observed. Thereby, the copper thin films are crystalline.
- ✓ The corroded films are uniform and compact and have a crystalline structure. The oxides operated like a protective layer against the aggressive environmental factor. This fact is confirmed by microscopical analyses.
- ✓ These material surfaces could be classified in very and perfect stable like as resistance group due to the linear shape of the cathodic and anodic branches. The H<sub>2</sub>SO<sub>4</sub> environment has the highest corrosion rate value. The HCl environment less corroded the surface and this fact means that the copper surface is passivated quickly. More corrosion resistant could be the CH<sub>3</sub>COOH solution.
- ✓ Thin and uniform copper layer appearance has a good capacity to reflect the light. The copper deposits tested in the acid solutions are opaque materials in VIS region due to the microelements from the surface.

#### References

- [1]. M. Schlesinger, M. Paunovic - *Modern Electroplating*, fourth ed., Wiley, New York, NY, (2000).
- [2]. A. Radisic, J.G. Long, P.M. Hoffmann, P.C. Searson - J. Electrochem. Soc. 148 (1), (2001), C41.
- [3]. G. Oskam, P.M. Vereecken, P.C. Searson - J. Electrochem. Soc. 146 (4), (1999), 1436.
- [4]. D. Grujicic, B. Pesic - *Electrodeposition of copper: the nucleation mechanisms*, Electrochim. Acta 47, (2002), 2901-2912.
- [5]. Aurbach D, Markovisky B et al - J. Power Sources 491:499, (2007).
- [6]. Xu J, Thomas HR et al - J. Power Sources 512-527 (2008).
- [7]. Searson PC, Ross FM et al - Surf. Sci. 1817-1826 (2006).
- [8]. Zangari G, Arrington D et al - Electrochim. Acta 2644-2649 (2008).
- [9]. Pasquale MA, Gassa LM et al - Electrochim. Acta 5891-5904 (2008).
- [10]. Gabrielli C, Devos O et al - J. Electroanal. Chem. 95-102 (2007).
- [11]. Nikolic ND, Brankovic G et al - J. Electroanal. Chem. 13-21 (2008).
- [12]. V. G. Celante, C. M. K. Pietre, C. M. B. J. G. Freitas - *Electrochemical and structural characterization of copper recycled from anodes of spent Li-ion batteries*, J. Appl. Electrochem. (2010) 40:23–28 DOI 10.1007/s10800-009-9959-2.
- [13]. D. Grujicic, B. Pesic - *Electrodeposition of copper: the nucleation mechanisms*, Department of Materials, Mining and Metallurgical Engineering and Geology, University of Idaho, McClure Hall, Moscow, ID 83844-3024, USA.
- [14]. A. Vicenzo, P.L. Cavallotti - Copper electrodeposition from a pH 3 sulfate electrolyte, J. Appl. Electrochem. 32: 743–753, (2002).
- [15]. A.M. Cantaragiu - *Studii si cercetari privind obtinerea si caracterizarea unor acoperiri nanostructurate biocompatibile*, PhD Thesis, (2011).
- [16]. D. Popovici, E. Trimbitasu, O. Pantea, D. Bombos, L. Antonescu - *Determinarea eficientei inhibitorului de coroziune Aticamina OTM 2 (The efficiency study of OTM2 Aticamina corrosion inhibitor)*, Buletinul Universitatii Petrol-Gaze din Ploiesti (Bulletin of the Petroleum-Gas University of Ploiesti), LIV, 4, 189-196, (2002).
- [17]. P. Hagioglu, C. Gheorghies, A.M. Cantaragiu, S. Moisa - *The Accelerated Corrosion Behaviour in Saline Environments of Some Samples Made of Tombac, Copper and Aluminium*, J. Sci. Arts, Year 20, 1(12), pp. 153-160, (2010), ISSN: 1844-9581, eISSN: 2068-3049.
- [18]. \*\*\* Joint Committee on Powder Diffraction Standards (1991) Diffraction Data File, No.45-0594, JCPDS international center for diffraction data, Pennsylvania.
- [19]. \*\*\* Joint Committee on Powder Diffraction Standards (1991) Diffraction Data File, No.5-661, JCPDS international center for diffraction data, Pennsylvania.
- [20]. P. Hagioglu, C. Gheorghies, A.M. Cantaragiu, R. Boiciuc, N. Tigau - *Corrosion Behaviour of Tombac Used in Cult Objects Manufacturing*, The Annals of "Dunarea de Jos" University of Galati, Fascicle IX, Metallurgy and Materials Sciences, 2, (2009), ISSN 1453-083X.